The diacylglycerol-binding protein α1-chimaerin regulates dendritic morphology

Philip Buttery*†‡, Asim A. Beg‡§, Ben Chih§, Arkady Broder§, Carol A. Mason*, and Peter Scheiffele§¶

*Department of Pathology and Cell Biology, Center for Neurobiology and Behavior, Columbia University, College of Physicians and Surgeons, P&S 14-509, 630 West 168th Street, New York, NY 10032; and §Department of Physiology and Cellular Biophysics, Center for Neurobiology and Behavior, Columbia University, College of Physicians and Surgeons, P&S 11-511, 630 West 168th Street, New York, NY 10032

Communicated by Thomas M. Jessell, Columbia University Medical Center, New York, NY, December 14, 2005 (received for review November 6, 2005)

The morphological and functional differentiation of neuronal dendrites is controlled through transcriptional programs and cell–cell signaling. Synaptic activity is thought to play an important role in the maturation of dendritic arbors, but the signaling pathways that couple neuronal activity and morphological changes in dendrites are not well understood. We explored the function of α1-chimaerin, a neuronal diacylglycerol-binding protein with a Rho GTPase-activating protein domain that inactivates Rac1. We find that stimulation of phospholipase Cβ-coupled cell surface receptors recruits α1-chimaerin to the plasma membrane of cultured hippocampal neurons. We further show that α1-chimaerin protein levels are controlled by synaptic activity and that increased α1-chimaerin expression results in the pruning of dendritic spines and branches. This pruning activity requires both the diacylglycerol-binding and Rac GTPase-activating protein activity of α1-chimaerin. Suppression of α1-chimaerin expression resulted in increased process growth from the dendritic shaft and from spine heads. Our data suggest that α1-chimaerin is an activity-regulated Rho GTPase regulator that is activated by phospholipase Cβ-coupled cell surface receptors and contributes to pruning of dendritic arbors.

spine | neuronal activity | phospholipase C | pruning

The pattern of neuronal connectivity in the mammalian central nervous system arises from an intricately choreographed sequence of developmental events, culminating in the outgrowth of neuronal processes, the assembly of synapses, and the formation of functional neuronal circuits. The shape of the dendritic arbor and distribution of dendritic spines are important determinants of afferent signal integration, and they are central to the structural and functional configuration of neuronal circuits (1).

Dendritic growth correlates developmentally with the arrival of afferent inputs, and evidence over many years has emphasized the importance of such input in stimulating dendritic growth (2). Most recently, live-imaging approaches have demonstrated that the normal mode of dendrite elaboration is synaptotropic, with afferent input acting both to increase branch dynamics and to stabilize individual branches (2–4). However, dendritic growth also requires regressive events that constrain dendritic expansion. Thus a dynamic balance exists between addition and elimination of individual dendritic protrusions, and the final arborization pattern is the product of thousands of independent local "decisions" to either stabilize or eliminate a particular branch. These decisions appear to be controlled by neuronal activity (5), but the mechanisms linking neural activity to growth and in particular to dendritic pruning are incompletely understood.

Rho GTPases are coordinators of the actin and microtubule cytoskeleton of all cell types (6). Rac, RhoA, and Cdc42, the primary members of this family, are central to regulating neuronal morphology, including the development of dendrites, and the formation and maintenance of spines and synapses (7). Activation of Rac results in the stabilization of synapses and dendritic branches. In contrast, RhoA drives dendritic retraction and the removal of spines (8–10). The activities of Rac and RhoA are balanced through crosstalk between these GTPases, and this balance of activities is thought to underlie neuronal process growth and retraction during development (11, 12).

GTP exchange factors (GEFs) and the GTPase-activating proteins (GAPs) are key signaling intermediates that convert cell surface signals into functional changes of Rho GTPase activity. GEFs activate GTPases by promoting GDP–GTP exchange, whereas GAPs stimulate GTP hydrolysis and thereby inactivate Rho GTPases. In developing neurons such GTPase regulators appear to be ideal candidate molecules for linking neurotransmitter receptor signaling to alterations in Rho protein activity (13, 14).

We have previously identified α-chimaerins as proteins whose genes were strongly up-regulated during the period of synaptogenesis (15). Studies in cell lines demonstrated that α-chimaerins have GAP activity toward Rac1 and to a lesser extent toward Cdc42 (16, 17). Moreover, α-chimaerins are members of an emerging family of non-PKC phorbol ester receptors that bind diacylglycerol (DAG) through a C1 domain (18). Chimaerins may therefore link lipid signaling and Rac inactivation.

From the α-chimaerin gene two isoforms, α1- and α2-chimaerin, are generated through alternative promoters (19). Both α-chimaerin isoforms contain C1 and Rho-GAP domains but they differ in that the α2 isoform contains an N-terminal SH2 domain that is absent from α1. The chimaerin isoforms also differ in their expression. α1-Chimaerin has been shown to be expressed in adult neurons (20, 21), whereas early neuronal expression has been reported for the α2 isoform. In this study, we show that α1-chimaerin expression in developing neurons is controlled by synaptic activity. The protein is rapidly recruited to the plasma membrane in response to generation of DAG downstream of phospholipase C (PLC)-linked receptors, where it mediates pruning of dendritic protrusions. Our findings suggest that α1-chimaerin may contribute to the activity-dependent regulation of dendritic growth during neuronal development.

Results

Regulation of α1-Chimaerin Expression. We previously identified α-chimaerins in a microarray analysis of the gene expression program underlying synaptic differentiation (15). To investigate α-chimaerin expression on the protein level, we raised α1- and α2-chimaerin isoform-specific antibodies (Fig. 1*A*) and performed a developmental Western blotting analysis on mouse hippocampal lysates. Levels of α1-chimaerin in hippocampal

Conflict of interest statement: No conflicts declared.

Abbreviations: DAG, diacylglycerol; GAP, GTPase-activating protein; mAChR, muscarinic acetylcholine receptor; mGluR, metabotropic glutamate receptor; PLC, phospholipase C; shRNA, small hairpin RNA.

†Present address: University of Cambridge Centre for Brain Repair, E. D. Adrian Building, Forvie Site, Robinson Way, Cambridge CB2 2PY, United Kingdom.

‡P.B. and A.A.B. contributed equally to this work.

¶To whom correspondence should be addressed. E-mail: ps2018@columbia.edu.

www.pnas.org/cgi/doi/10.1073/pnas.0510655103

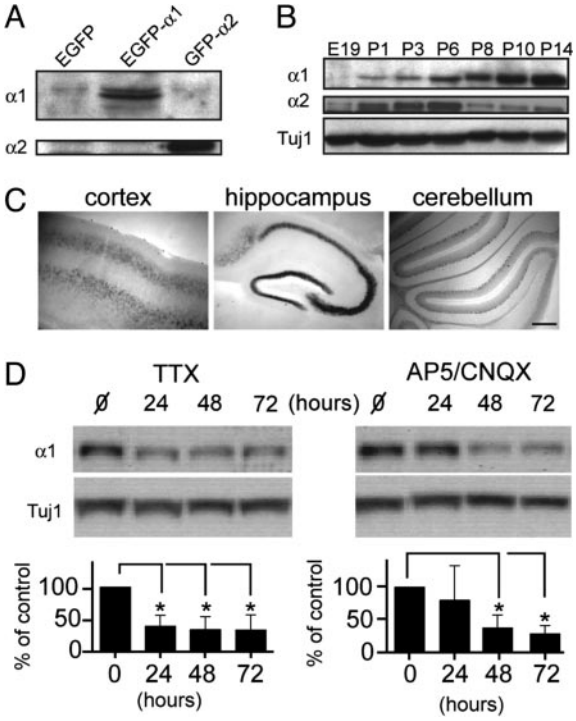

Fig. 1. Expression of α1-chimaerin. (*A*) Lysates from HEK 293 cells expressing EGFP, EGFP-α1-chimaerin, or EGFP-α2-chimaerin were probed with α1- and α2-specific antibodies. (*B*) Lysates from rat hippocampal tissue [embryonic day 19 (E19) through postnatal day 14 (P14)] were analyzed with α-chimaerin isoform-specific antibodies. (*C*) *In situ* hybridization on cortical, hippocampal, and cerebellar mouse tissue at postnatal day 10. No labeling was seen with sense probes (not shown). (Scale bar, 200 μm.) (*D*) (*Upper*) Western blot analysis with α1-specific antibodies on lysates from hippocampal cultures exposed to either tetrodotoxin (TTX) (1.5 μM), or 2-amino-5-phosphonopentanoic acid (AP5, 50 μM) and 6-cyano-7-nitroquinoxaline-2,3-dione (CNQX, 10 μM). (*Lower*) Relative protein levels were quantified by densitometric scanning ($n = 3$; *, $P < 0.05$).

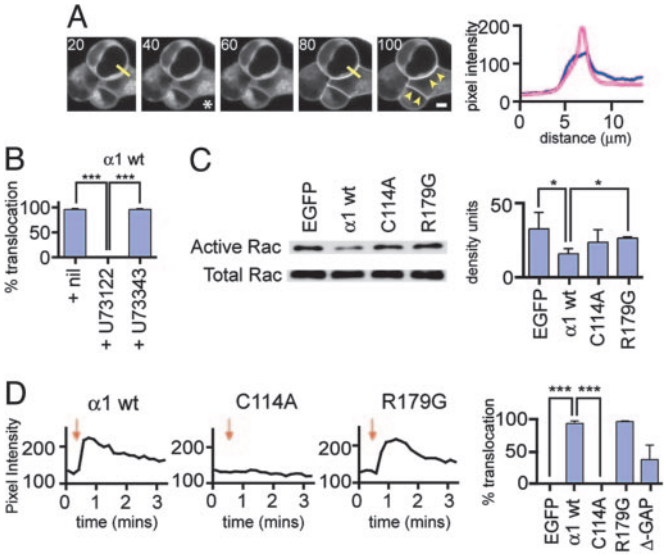

Fig. 2. EGFP-α1-chimaerin recruitment in response to DAG signaling. (*A*) (*Left*) Time-lapse microscopy of HEK 293 cells expressing mAChR1 and EGFP-α1-chimaerin-R179G. The asterisk marks time of stimulation with 5 mM carbachol. (*Right*) Intensity plot through cell junction (yellow line), before (blue) and 40 sec after stimulation (pink). (Scale bar, 5 μm.) (*B*) The percentage of cells exhibiting translocation was scored for control conditions compared with presence of either U73122 (20 μM) or U73343 (20 μM). The result is the mean of three independent experiments; ***, $P < 0.0005$. (*C*) Point mutations in the C1 (C114A) and GAP (R179G) domains of α1-chimaerin result in decreased Rac-GAP activity as measured by PAK1 CRIB-domain pull-down assays in HEK 293 cells. Active and total Rac1 were detected by Western blotting (*Left*), and quantitated (*Right*) ($n = 3$; *, $P < 0.05$). (*D*) (*Left*) Translocation of wild-type and mutant EGFP-α1-chimaerins shown as the peak fluorescence intensity at the site of cell–cell junctions. Frames were captured every 10 sec, and red arrows mark the addition of carbachol. (*Right*) Percentage of cells exhibiting translocation (*, $P < 0.05$).

tissue slowly increased during the first 2 weeks of postnatal development, whereas α2-chimaerin protein levels peaked around postnatal day 6 and declined thereafter (Fig. 1*B*). *In situ* hybridization on postnatal day 10 revealed high α1-chimaerin expression in neurons of the hippocampus and cortex, as well as in Purkinje cells in the cerebellum (Fig. 1*C*). Because Purkinje cells and hippocampal neurons expressed particularly high levels of α1-chimaerin, we chose these two neuronal cell types for further study of α1-chimaerin regulation and function.

Cultured hippocampal neurons showed a developmental increase of α1-chimaerin expression similar to the one observed *in vivo* (data not shown). To determine whether neuronal activity contributes to the dynamic regulation of α1-chimaerin expression, we blocked sodium channel-dependent action potentials by application of tetrodotoxin (TTX), or α-amino-3-hydroxy-5-methyl-4-isoxazolepropionic acid (AMPA)- and *N*-methyl-D-aspartate (NMDA)-receptor activity by application of 6-cyano-7-nitroquinoxaline-2,3-dione (CNQX) and 2-amino-5-phosphonopentanoic acid (AP5). Protein expression of α1-chimaerin was highly sensitive to activity blockade, showing a >60% decrease after 48 h of pharmacological blockade under either condition (Fig. 1*D*). Therefore, α1-chimaerin is a neuronal Rac-GAP protein that is regulated by neuronal activity.

Activation of PLCβ-Coupled Receptors Recruits α1-Chimaerin. α1-Chimaerin contains a C1 domain that binds to phorbol esters and DAG *in vitro* (22). To test whether DAG signaling in intact cells affects α1-chimaerin distribution we performed time-lapse imaging of an EGFP-α1-chimaerin fusion protein in HEK 293 cells, which express the muscarinic acetylcholine receptor 1 (mAChR1), a cell surface receptor that couples to PLCβ and produces DAG upon activation. When cells were stimulated with the mAChR agonist carbachol, we observed translocation of α1-chimaerin from an intracellular pool to the plasma membrane over a time course of seconds (Fig. 2*A*). Line scans through the cell cytoplasm and plasma membrane revealed a selective increase in fluorescence at the plasma membrane, suggesting direct translocation of EGFP-α1-chimaerin to the plasma membrane. To confirm that the translocation required PLCβ activation we preincubated HEK 293 cells with the PLCβ inhibitor U73122 or the inactive derivative U73343, and then applied carbachol. PLCβ inhibition with U73122 abolished EGFP-α1-chimaerin translocation, whereas the inactive derivative U73343 had no effect (Fig. 2*B*).

We next examined the importance of the C1 and GAP domains of α1-chimaerin in DAG-dependent translocation. To this end we generated three mutant proteins: one containing a point mutation in the C1 domain that disrupts phorbol-ester binding (C114A) (23); one containing a point mutation in the GAP domain (R179G) that abolishes Rac-GAP activity (21, 24); and a deletion mutant in which the entire GAP domain was deleted (ΔGAP). To confirm Rac-GAP activity of the two point mutants we performed GTPase pull-down assays with the Rac effector (CRIB) domain of the serine/threonine kinase PAK1, which selectively affinity purifies the GTP-bound form of Rac (Fig. 2*C*). Whereas wild-type α1-chimaerin reduced the levels of bound active Rac, the R179G mutant did not alter the amount

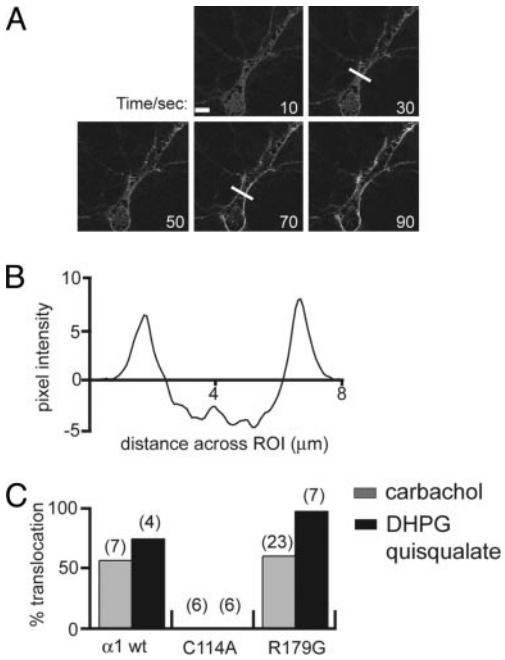

Fig. 3. Plasma membrane translocation of α1-chimaerin in hippocampal neurons. (*A*) Frames from a representative time-lapse series of a hippocampal neuron transfected with EGFP-α1-chimaerin-R179G and stimulated with carbachol (5 mM). Frames are shown after digital subtraction from the first frame. (*B*) Line scan of fluorescence intensity change from frame acquired at 30 and 70 sec (white line in *A*). (*C*) Percentage of cells exhibiting translocation to the plasma membrane upon stimulation with carbachol (5 mM, gray bars) or with the metabotropic glutamate receptor (mGluR) agonists (*S*)-3,5-dihydroxyphenylglycine (DHPG) or quisqualate (200 μM and 250 μM, respectively, black bars). Numbers in parentheses give total number of observations.

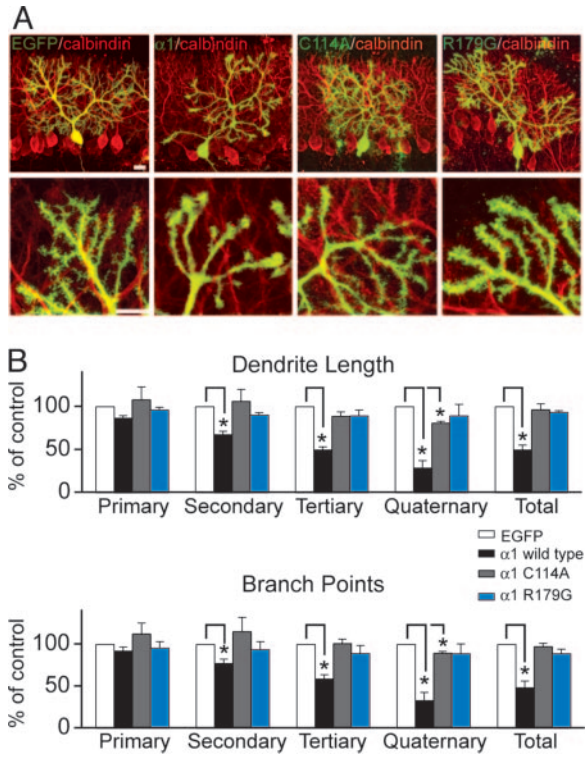

Fig. 4. Effect of α1-chimaerin on dendritic arbors and dendritic spines. (*A*) Purkinje cells in cerebellar slices were transfected with EGFP and wild-type or each of the two mutant EGFP-α1-chimaerins. All Purkinje cells are labeled for EGFP (green) and calbindin (red). (Scale bars, 20 μm.) (*B*) Quantitation of total dendritic length (*Upper*) and dendritic branch points (*Lower*) in wild-type and mutant α1-chimaerin-expressing Purkinje cells ($n > 10$ cells; *, $P > 0.05$).

of active Rac as compared with control cells. The C114A mutation in the C1 domain yielded intermediate results, indicating that DAG binding may be required for full GAP activity, as previously suggested (16).

We then tested plasma membrane recruitment of wild-type and mutant versions of EGFP-α1-chimaerin in response to mAChR1 stimulation (Fig. 2*D*). The C114A mutation in the C1 domain abolished translocation, whereas inactivation of the GAP activity by the R179G mutation had no dramatic effect. This finding indicates that the C1 domain is required and sufficient for DAG-induced plasma membrane translocation of α1-chimaerin in heterologous cells.

Finally, we examined whether plasma membrane recruitment of α1-chimaerin is observed in response to stimulation of endogenous cell surface receptors in primary neurons. EGFP-α1-chimaerin or the mutant proteins were transfected into cultured hippocampal neurons and observed by time-lapse confocal microscopy (Fig. 3). Hippocampal neurons express significant levels of mAChRs and metabotropic glutamate receptors (mGluRs), which couple to PLCβ. When mAChRs were stimulated with carbachol, EGFP-α1-chimaerin exhibited rapid translocation to the membrane over a time-course similar to that observed in HEK 293 cells. Translocation with muscarinic agonist was seen with both wild-type and R179G mutant α1-chimaerin, but not with the C114A mutant (Fig. 3*B*). Translocation was also observed with the metabotropic glutamate receptor (mGluR) agonists (*S*)-3,5-dihydroxyphenylglycine (DHPG, 200 μM) or quisqualate (250 μM). In summary, these results suggest that α1-chimaerin is a functional DAG receptor that is recruited to the plasma membrane in response to activation of PLCβ-coupled cell surface receptors in neurons.

α1-Chimaerin Promotes Pruning of Dendritic Branches and Spines. Our expression analysis revealed that cellular α1-chimaerin levels are tightly regulated by neuronal activity (Fig. 1*D*). To investigate the cellular consequences of altered α1-chimaerin expression, we elevated α1-chimaerin levels by overexpression in neurons. We initially focused this analysis on cerebellar Purkinje cells, because these cells normally express α1-chimaerin but no detectable levels of other chimaerin isoforms.

Overexpression of α1-chimaerin in Purkinje cells in organotypic slice cultures resulted in a dramatic alteration of dendritic morphology (Fig. 4*A*). There was a reproducible simplification and pruning of the dendritic arbor, associated with "clubbing" of the distal dendritic tips and loss of normal spines. Morphometric analysis revealed an $\approx$50% reduction in dendritic length and branch point number, with most severe effects in higher-order branches (Fig. 4*B*). In addition, we measured dendritic height for comparison with surrounding untransfected cells in the same microscope field. No significant difference was observed, indicating that the action of α1-chimaerin is cell autonomous (dendritic height of untransfected cells was 149 $\pm$ 7 μm in slices with EGFP-transfected cells and 147 $\pm$ 4 μm in slices with α1-chimaerin-expressing cells). To understand the respective contribution of the C1 and GAP domains to the retraction phenotype we expressed the C114A and R179G mutants. Both the DAG-binding site and GAP activity of the protein were required for the induction of dendritic pruning (Fig. 4).

A similar pruning activity of α1-chimaerin was also observed when the protein was expressed in cultured hippocampal neurons, indicating that the retraction pathway is shared between these two cells types (Fig. 5). Hippocampal neurons also express the α2 isoform, which differs from α1-chimaerin by the presence

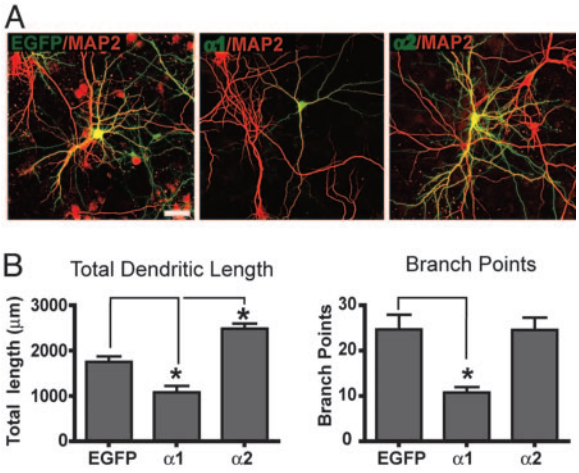

Fig. 5. Overexpression of α-chimaerins in dissociated hippocampal neurons. (*A*) Dissociated hippocampal neurons were transfected at 10 days *in vitro* with EGFP, EGFP-α1-chimaerin, or EGFP-α2-chimaerin and labeled with EGFP (green) and microtubule-associated protein 2 (red) antibodies. (Scale bar, 40 μm.) (*B*) Quantitation of total dendritic length and number of branch points ($n > 10$ cells; *, $P < 0.05$).

of an N-terminal SH2 domain. In contrast to α1-chimaerin, the α2 isoform did not induce dendritic pruning when overexpressed, but it significantly increased process outgrowth (Fig. 5). These findings suggest that α1-chimaerin regulates dendritic morphology in Purkinje and hippocampal neurons by coupling DAG signaling and Rac inactivation and that the presence of an SH2 domain in α2-chimaerin differentially regulates this function.

α1-Chimaerin Inhibits Dendritic Protrusions. To define essential functions for α1-chimaerin in regulating dendritic morphology, we used an RNA interference approach. We designed expression constructs for small hairpin RNAs (shRNAs) based on α1-specific regions of the α-chimaerin transcript. The efficiency of α1-chimaerin suppression was measured in cultured hippocampal neurons because these cells are more accessible for biochemical analysis than Purkinje cells. Two of the selected shRNA sequences (sh1 and sh2) produced >90% knockdown of endogenous α1-chimaerin when delivered with recombinant lentiviruses into cultured hippocampal neurons (Fig. 6*A*). Vectors lacking an shRNA insert or containing a control shRNA did not alter α1-chimaerin levels. The specificity of α1-chimaerin down-regulation was confirmed by introducing point mutations into one of the functional shRNA sequences. These mutant shRNAs (sh2m1 and sh2m2) failed to suppress α1-chimaerin expression. Finally, we monitored levels of the α2-chimaerin isoform in cells expressing the α1-chimaerin shRNAs and found that α2-chimaerin levels were not altered. This finding demonstrates that the selected shRNAs mediate efficient and specific suppression of endogenous α1-chimaerin in hippocampal neurons.

For morphological analysis shRNAs were introduced into dissociated hippocampal neurons and pyramidal neurons in organotypic slices of rat hippocampus. In both culture systems the two active hairpin constructs produced essentially identical phenotypes. Down-regulation of α1-chimaerin increased protrusive activity from the dendrite (Fig. 6). Interestingly, the total number of dendritic protrusions was not altered, but the number of normal headed spines per unit length of dendrite was decreased by $\approx$50% as compared with control cells or cells transfected with the mutant shRNAs. At the same time there was an increase in filopodial-type protrusions and spine structures

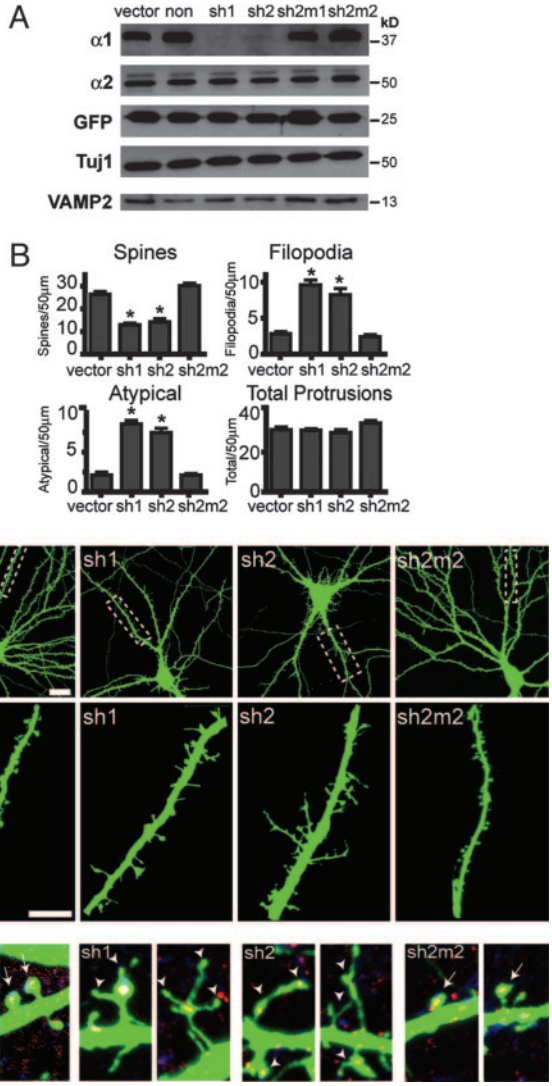

Fig. 6. Suppression of α1-chimaerin in hippocampal neurons results in excess outgrowth of dendritic protrusions. (*A*) Dissociated hippocampal neurons were infected with lentiviral vectors encoding shRNAs targeted against α1-chimaerin (sh1 and sh2), with mutated shRNAs (sh2m1 and sh2m2), with lentiviruses lacking an shRNA insert (vector), or with an active control hairpin (''non,'' against p53). Lysates were probed with antibodies against α1-chimaerin, α2-chimaerin, Tuj1, and VAMP2. Comparable viral infection was confirmed by probing for EGFP, which was coexpressed with the shRNAs. (*B* and *C*) Morphometric analysis (*B*) and representative images (*C*) from hippocampal neurons transfected with control, sh1, sh2, and sh2m2 shRNA vectors ($n > 10$ cells; *, $P < 0.05$). (Scale bars, 20 μm and 10 μm for the whole-cell images and the enlarged region, respectively.) (*D*) Spine phenotypes from control and knockdown cells. Control and sh2m2 cells exhibited normal stubby and mushroom-headed spines (arrows); whereas, sh1 and sh2 cells show an increase in atypical spines with filopodia emanating from the spine head (arrowheads). PSD-95 (red) and VGLUT1 (blue) staining visualize synaptic terminals.

with multiple protrusions emerging directly from spine heads. These atypical spine structures remained associated with synaptic terminals as indicated by immunostaining for the synaptic vesicle marker synaptobrevin and the postsynaptic scaffolding molecule PSD95, and frequently single spine-like protrusions carried multiple synaptic contacts (Fig. 6*C*). This phenotype suggests that the endogenous α1-chimaerin acts to limit the expansion of dendritic protrusions and thereby contributes to the normal development of dendritic arbors.

Discussion

Our analysis of α1-chimaerin leads to the following conclusions: (*i*) α1-chimaerin expression is regulated by neuronal activity; (*ii*) α1-chimaerin is recruited in response to activation of PLCβ-coupled cell surface receptors, and (*iii*) α1-chimaerin drives pruning of dendritic protrusions through a mechanism that requires the DAG-binding domain.

These findings implicate α1-chimaerin as a previously unrecognized player in the activity-dependent regulation of dendritic development. In contrast with several previously identified signaling molecules, α1-chimaerin contributes to pruning rather than elaboration of dendrites. For example, the NR2B-associated Rac–GTP exchange factor (GEF) Tiam1 leads to Rac activation and spine growth in response to NMDA-receptor stimulation (14). Two other previously characterized GEFs, kallirin and intersectin, are recruited by EphB receptors, activate Rac and Cdc42, and thereby promote the formation of dendritic protrusions (25–27). α1-Chimaerin might act to counterbalance such activities by inactivating Rac1 and thereby limiting the growth of dendritic arbors. The main role for α1-chimaerin in this process is likely at the level of the dendritic spines because our loss of function experiments revealed filopodial overgrowth from dendrites. In the overexpression studies we observed not only spine retraction but also pruning of entire dendritic branches. It remains to be shown whether long-term loss of α1-chimaerin results in excessive branching or whether the pruning of branches in the gain-of-function condition is due to global effects caused by overexpression.

Chimaerin function is regulated at multiple levels. First, we observed down-regulation of α1-chimaerin in response to neuronal activity blockade. Previous studies have reported dendritic growth and neuronal activity to be directly correlated (2, 28). In this context the down-regulation of α1-chimaerin in response to reduced neuronal activity might represent a cell-wide homeostatic response to limit its pruning activity under conditions of limited dendritic growth. Second, pruning activity requires active DAG signaling. PLCβ-dependent DAG generation might determine the subcellular localization of α1-chimaerin action or alternatively the duration of its activity. A third mechanism for α1-chimaerin regulation is suggested by the differing activities of the α1- and α2-chimaerin isoforms. Both isoforms have identical C1 and Rac-GAP domain sequences, but α2-chimaerin contains an additional N-terminal SH2 domain. We have shown that α2-chimaerin promotes neuronal process growth rather than pruning. This dramatic functional difference between the two isoforms may result from direct regulation of the GAP activity by intramolecular interactions or from differential subcellular localization and function by means of the SH2 domain. Further studies focusing on α2-chimaerin will be required to clarify this opposing mechanism.

Our findings regarding α1-chimaerin complement work by VanDongen and colleagues, who suggested that α1-chimaerin can promote the removal of dendritic spines from dissociated hippocampal neurons (29). Whereas our results demonstrate that the DAG-binding site in α1-chimaerin is essential for membrane recruitment in response to PLCβ activation, VanDongen and colleagues suggested that in hippocampal neurons the C terminus of α1-chimaerin binds directly to the NR2A subunit of NMDA receptors in a phorbol ester-dependent manner (29). DAG signaling might initiate α1-chimaerin activation and recruitment to NR2A-containing sites, thus resulting in local inactivation of Rac1. However, further work is required to clarify which cell surface receptors act upstream of α1-chimaerin. We observed similar dendritic pruning activities for overexpressed α1-chimaerin in Purkinje cells and hippocampal neurons. Interestingly, Purkinje cells do not express functional NMDA receptors and only very low levels of NR2A (30–32). Therefore, α1-chimaerin most likely acts independently of NR2A in these cells.

Our imaging studies revealed that activation of both mAChR1 and group I mGluRs with specific agonists resulted in plasma membrane translocation of α1-chimaerin, which was abolished by inhibition of PLCβ (Figs. 3 and 4). Signaling downstream of mGluRs and PLCβ represents an attractive model for α1-chimaerin function because there is substantial evidence supporting a role for group I mGluR activation in dendritic development and plasticity (33). Mice lacking mGluR1 show impaired long-term depression in the hippocampus and in cerebellar Purkinje cells, which express high levels of α1-chimaerin (34). Moreover, mGluR5 and PLCβ1 mutant mice show defects in activity-dependent differentiation of the barrel structure in the somatosensory cortex (35). Additionally, dendritic spines in PLCβ1 mutants have atypical morphologies reminiscent of the α1-chimaerin loss-of-function phenotype that we observed in hippocampal slice cultures (36).

Exuberant spine growth and atypical spine structures have also been observed in developing tissues, suggesting that they may represent immature or developing dendritic structures (37, 38). In developing CA1 neurons, motility of dendritic protrusions appears to decrease once contacts with presynaptic terminals are established (39). The increase of atypical spines with protrusions in neurons lacking α1-chimaerin may therefore reflect a role for α1-chimaerin in the maturation step that leads to the formation of stable spine structures.

Because α1-chimaerin continues to be expressed in the adult brain (20, 21) its function does not appear to be restricted to developing neurons. In the future it will be interesting to explore whether α1-chimaerin also contributes to the ongoing addition and elimination of synapses in response to environmental input and synaptic activity (40, 41).

Materials and Methods

DNA Vectors. α1- and α2-chimaerin cDNAs obtained by PCR amplification from EST clones (BG695071, AI194286, BI248665) were inserted into the pEGFP-C1 vector (Clontech) for N-terminal EGFP tagging. Mutants C114A and R179G were created by site-directed mutagenesis (QuickChange; Stratagene). In the deletion mutant ΔGAP the α1-chimaerin coding sequence was truncated at amino acid 171. Primers for probes for *in situ* hybridization were 5′-GGGAGGAAAGCTAACAGAGC-3′ and 5′-TCAACTGCGAATAGGCAAAGA-3′. Hybridization with digoxigenin-labeled RNA probes was performed as described in ref. 42. Expression vectors generously provided by other researchers were human mAChR1 (Sven-Eric Jordt, Yale University, New Haven, CT) and Pak1-CRIB domain (Linda Van Aelst, Cold Spring Harbor Laboratory, Cold Spring Harbor, NY).

Antibodies. The following primary antibodies were used: rabbit anti-EGFP (Molecular Probes), mouse anti-Rac1 (23A8; Upstate Biotechnology, Lake Placid, NY), mouse anti-βIII-tubulin (Tuj1; Covance, Princeton, NJ), mouse and rat anti-hemagglutinin epitope (HA) tag (12CA5 and 4F10; Roche Biosciences), mouse anti-VAMP2 (Synaptic Systems, Goettingen, Germany), and mouse anti-MAP2 (Chemicon International, Temecula, CA). Polyclonal antibodies against α1- and α2-chimaerin were raised in rabbits immunized with keyhole limpet hemocyanin-coupled synthetic peptides (α1-chimaerin, MPSKESWSGRKANR; α2-chimaerin, HDEKEATGQDGVSEKR). Sera were affinity purified on immobilized peptides. Secondary antibodies were from Jackson ImmunoResearch and Molecular Probes.

Lentiviral Vectors and shRNAs. shRNA cloning and lentiviral production were as described in refs. 43 and 44, using a modified

version of the LenLox3.7 vector in which EGFP expression is driven by the β-actin promoter. Neurons were analyzed 6 days after viral infection. Target sequences in α1-chimaerin were as follows: sh1, 5′-CTAATAGAGCTACAGTTCA-3′; sh2, 5′-GCTTTCAGCAATGTGTCAT-3′; sh2m1, 5′-GCTTTCAGCATTGTGTCAT-3′; and sh2m2, 5′-GCTTTCAGCATTGTGACAT-3′.

Primary Neuronal Cultures. Parasagittal cerebellar slices (250 μm) prepared from postnatal day 10 mice by using a McIlwain tissue chopper were cultured on Millicell 0.4-μm culture inserts (Millipore PICM 03050) and transfected by biolistic particle-mediated delivery (Bio-Rad hand-held gene gun) as described in ref. 45. Slices were fixed and analyzed at 24 h after transfection. Hippocampal slices (350 μm) were prepared from postnatal day 5–6 rats and cultured on 0.4-μm Millicell membranes (Millipore PICMORG 50). At 5 days *in vitro*, slices were biolistically transfected, and 6 days later they were analyzed. Culture and transfection of dissociated hippocampal cells were as described in refs. 44 and 46). For shRNA knockdown, cells were transfected with 50 ng of plasmid DNA and analyzed 6 days after transfection.

Image Acquisition and Analysis. Image stacks of 10 randomly chosen cells collected on a Zeiss LSM 510 scanning confocal microscope were analyzed by using IMAGEJ and OBJECT IMAGE software (http://rsb.info.nih.gov/ij/). Image stacks were collapsed into a single 2D frame and imported into OBJECT IMAGE. Dendritic parameters were assessed by using a modification of the method described by Ruthazer and Cline (47). The number of protrusions and spine types was quantitated for 50-μm segments of at least 10 cells for four independent experiments. Total protrusion numbers were counted and subclassified into normal spines, atypical spines, and filopodia. Figures for all experiments show SEM, and one-way ANOVA was used to assess statistical significance.

Live images of HEK 293 cells expressing EGFP-α1-chimaerin were collected in 10-sec intervals on a Zeiss LSM 510 laser scanning confocal microscope. For hippocampal neurons, cells were transfected at 12–13 days *in vitro* and analyzed 24–48 h later.

We are grateful to Drs. Linda Van Aelst, Marcelo Kazanietz, and Sven-Eric Jordt for providing DNA constructs; Dr. Gilbert DiPaolo and Mari Takasu for comments on the manuscript; and Gregg Gundersen for discussion. This work was financially supported by a Wellcome Trust Intermediate Fellowship and a postdoctoral fellowship from the National Alliance for Autism Research (to P.B.), a postdoctoral fellowship from the American Cancer Society and a National Institutes of Health Training grant (to A.A.B.), National Institutes of Health Grant NS16951 (to C.A.M.), a pilot grant from the Alzheimer's Disease Research Center at Columbia University, and grants from the Irma T. Hirschl Trust and the Searle Scholar Program (to P.S.).

1. Bonhoeffer, T. & Yuste, R. (2002) *Neuron* **35,** 1019–1027.
2. Wong, R. O. & Ghosh, A. (2002) *Nat. Rev. Neurosci.* **3,** 803–812.
3. Niell, C. M., Meyer, M. P. & Smith, S. J. (2004) *Nat. Neurosci.* **7,** 254–260.
4. Sin, W. C., Haas, K., Ruthazer, E. S. & Cline, H. T. (2002) *Nature* **419,** 475–480.
5. Hua, J. Y., Smear, M. C., Baier, H. & Smith, S. J. (2005) *Nature* **434,** 1022–1026.
6. Hall, A. & Nobes, C. D. (2000) *Philos. Trans. R. Soc. London B* **355,** 965–970.
7. Van Aelst, L. & Cline, H. T. (2004) *Curr. Opin. Neurobiol.* **14,** 297–304.
8. Threadgill, R., Bobb, K. & Ghosh, A. (1997) *Neuron* **19,** 625–634.
9. Nakayama, A. Y., Harms, M. B. & Luo, L. (2000) *J. Neurosci.* **20,** 5329–5338.
10. Tashiro, A., Minden, A. & Yuste, R. (2000) *Cereb. Cortex* **10,** 927–938.
11. Li, Z., Van Aelst, L. & Cline, H. T. (2000) *Nat. Neurosci.* **3,** 217–225.
12. Li, Z., Aizenman, C. D. & Cline, H. T. (2002) *Neuron* **33,** 741–750.
13. Govek, E. E., Newey, S. E., Akerman, C. J., Cross, J. R., Van der Veken, L. & Van Aelst, L. (2004) *Nat. Neurosci.* **7,** 364–372.
14. Tolias, K. F., Bikoff, J. B., Burette, A., Paradis, S., Harrar, D., Tavazoie, S., Weinberg, R. J. & Greenberg, M. E. (2005) *Neuron* **45,** 525–538.
15. Diaz, E., Ge, Y., Yang, Y. H., Loh, K. C., Serafini, T. A., Okazaki, Y., Hayashizaki, Y., Speed, T. P., Ngai, J. & Scheiffele, P. (2002) *Neuron* **36,** 417–434.
16. Ahmed, S., Kozma, R., Hall, C. & Lim, L. (1995) *Methods Enzymol.* **256,** 114–125.
17. Caloca, M. J., Wang, H. W. & Kazanietz, M. G. (2003) *Biochem. J.* **375,** 313–321.
18. Brose, N., Betz, A. & Wegmeyer, H. (2004) *Curr. Opin. Neurobiol.* **14,** 328–340.
19. Dong, J. M., Smith, P., Hall, C. & Lim, L. (1995) *Eur. J. Biochem.* **227,** 636–646.
20. Lim, H. H., Michael, G. J., Smith, P., Lim, L. & Hall, C. (1992) *Biochem. J.* **287,** 415–422.
21. Hall, C., Michael, G. J., Cann, N., Ferrari, G., Teo, M., Jacobs, T., Monfries, C. & Lim, L. (2001) *J. Neurosci.* **21,** 5191–5202.
22. Ahmed, S., Kozma, R., Monfries, C., Hall, C., Lim, H. H., Smith, P. & Lim, L. (1990) *Biochem. J.* **272,** 767–773.
23. Caloca, M. J., Garcia-Bermejo, M. L., Blumberg, P. M., Lewin, N. E., Kremmer, E., Mischak, H., Wang, S., Nacro, K., Bienfait, B., Marquez, V. E. & Kazanietz, M. G. (1999) *Proc. Natl. Acad. Sci. USA* **96,** 11854–11859.
24. Ahmed, S., Lee, J., Wen, L. P., Zhao, Z., Ho, J., Best, A., Kozma, R. & Lim, L. (1994) *J. Biol. Chem.* **269,** 17642–17648.
25. Irie, F. & Yamaguchi, Y. (2002) *Nat. Neurosci.* **5,** 1117–1118.
26. Penzes, P., Beeser, A., Chernoff, J., Schiller, M. R., Eipper, B. A., Mains, R. E. & Huganir, R. L. (2003) *Neuron* **37,** 263–274.
27. Ma, X. M., Huang, J., Wang, Y., Eipper, B. A. & Mains, R. E. (2003) *J. Neurosci.* **23,** 10593–10603.
28. Redmond, L., Kashani, A. H. & Ghosh, A. (2002) *Neuron* **34,** 999–1010.
29. Van de Ven, T. J., VanDongen, H. M. A. & VanDongen, A. M. J. (2005) *J. Neurosci.* **25,** 9488–9496.
30. Kano, M. & Kato, M. (1987) *Nature* **325,** 276–279.
31. Hausser, M. & Roth, A. (1997) *J. Physiol.* **501,** 77–95.
32. Thompson, C. L., Drewery, D. L., Atkins, H. D., Stephenson, F. A. & Chazot, P. L. (2000) *Neurosci. Lett.* **283,** 85–88.
33. Malenka, R. C. & Bear, M. F. (2004) *Neuron* **44,** 5–21.
34. Aiba, A., Kano, M., Chen, C., Stanton, M. E., Fox, G. D., Herrup, K., Zwingman, T. A. & Tonegawa, S. (1994) *Cell* **79,** 377–388.
35. Hannan, A. J., Blakemore, C., Katsnelson, A., Vitalis, T., Huber, K. M., Bear, M., Roder, J., Kim, D., Shin, H. S. & Kind, P. C. (2001) *Nat. Neurosci.* **4,** 282–288.
36. Spires, T. L., Molnar, Z., Kind, P. C., Cordery, P. M., Upton, A. L., Blakemore, C. & Hannan, A. J. (2005) *Cereb. Cortex* **15,** 385–393.
37. Mason, C. A. (1983) *J. Comp. Neurol.* **217,** 458–469.
38. Fiala, J. C., Feinberg, M., Popov, V. & Harris, K. M. (1998) *J. Neurosci.* **18,** 8900–8911.
39. Konur, S. & Yuste, R. (2004) *Mol. Cell Neurosci.* **27,** 427–440.
40. Grutzendler, J., Kasthuri, N. & Gan, W. B. (2002) *Nature* **420,** 812–816.
41. Trachtenberg, J. T., Chen, B. E., Knott, G. W., Feng, G., Sanes, J. R., Welker, E. & Svoboda, K. (2002) *Nature* **420,** 788–794.
42. Schaeren-Wiemers, N. & Gerfin-Moser, A. (1993) *Histochemistry* **100,** 431–440.
43. Reynolds, A., Leake, D., Boese, Q., Scaringe, S., Marshall, W. S. & Khvorova, A. (2004) *Nat. Biotechnol.* **22,** 326–330.
44. Chih, B., Engelman, H. & Scheiffele, P. (2005) *Science* **307,** 1324–1328.
45. Dunaevsky, A., Tashiro, A., Majewska, A., Mason, C. & Yuste, R. (1999) *Proc. Natl. Acad. Sci. USA* **96,** 13438–13443.
46. Dean, C., Scholl, F. G., Choih, J., DeMaria, S., Berger, J., Isacoff, E. & Scheiffele, P. (2003) *Nat. Neurosci.* **6,** 708–716.
47. Ruthazer, E. S. & Cline, H. T. (2002) *Real-Time Imaging* **8,** 175–188.